Purine Nucleoside Phosphorylase from *Mycobacterium tuberculosis*. Analysis of Inhibition by a Transition-State Analogue and Dissection by Parts†

Luiz A. Basso,‡ Diogenes S. Santos,‡ Wuxian Shi,§ Richard H. Furneaux,|| Peter C. Tyler,|| Vern L. Schramm,§ and John S. Blanchard*,§

Department of Biochemistry, Albert Einstein College of Medicine, 1300 Morris Park Avenue, Bronx, New York 10461, Departamento de Biologia Molecular e Biotecnologia, Universidade Federal do Rio Grande do Sul, Avenida Bento Gonçalves 9500, Porto Alegre-RS 91501-970, Brazil, and Carbohydrate Chemistry Team, Industrial Research, Ltd., Lower Hutt, New Zealand

Received March 23, 2001; Revised Manuscript Received May 14, 2001

ABSTRACT: Purine salvage pathways are predicted to be present from the genome sequence of *Mycobacterium tuberculosis*. The *M. tuberculosis deoD* gene encodes a presumptive purine nucleoside phosphorylase (PNP). The gene was cloned, expressed, purified, and found to exhibit PNP activity. Purified *M. tuberculosis* PNP is trimeric, similar to mammalian PNP's but unlike the hexameric *Escherichia coli* enzyme. Immucillin-H is a rationally designed analogue of the transition state that has been shown to be a potent inhibitor of mammalian PNP's. This inhibitor also exhibits slow-onset inhibition of *M. tuberculosis* PNP with a rapid, reversible inhibitor binding (K_i of 2.2 nM) followed by an overall dissociation constant (K_i*) of 28 pM, yielding a K_m/K_i* value of 10^6. Time-dependent tight binding of the inhibitor occurs with a rate of 0.1 s^{-1}, while relaxation of the complex is slower at 1.4×10^{-3} s^{-1}. The pH dependence of the K_i value of immucillin-H to the *M. tuberculosis* PNP suggests that the inhibitor binds as the neutral, unprotonated form that is subsequently protonated to generate the tight-binding species. The *M. tuberculosis* enzyme demonstrates independent and equivalent binding of immucilin-H at each of the three catalytic sites, unlike mammalian PNP. Analysis of the components of immucillin-H confirms that the inhibition gains most of its binding energy from the 9-deazahypoxanthine group (K_{is} of 0.39 μM) while the 1,4-dideoxy-1,4-iminoribitol binds weakly (K_{is} of 2.9 mM). Double-inhibition studies demonstrate antagonistic binding of 9-deazahypoxanthine and iminoribitol ($\beta = 13$). However, the covalent attachment of these two components in immucillin-H increases equilibrium binding affinity by a factor of >14 000 (28 pM vs 0.39 μM) compared to 9-deazahypoxanthine alone, and by a factor of $>10^8$ compared to iminoribitol alone (28 pM vs 2.9 mM), from initial velocity measurements. The structural basis for *M. tuberculosis* PNP inhibition by immucillin-H and by its component parts is reported in the following paper [Shi, W., Basso, L. A., Santos, D. S., Tyler, P. C., Furneaux, R. H., Blanchard, J. S., Almo, S. C., and Schramm, V. L. (2001) *Biochemistry 40,* 8204−8215].

The World Health Organization (WHO) has declared tuberculosis (TB) to be a global emergency (*1*). Tuberculosis resurged in the late 1980s and now kills more than 2 million people a year, second only to AIDS among infectious diseases (*2*). The high susceptibility of human immunodeficiency virus-infected persons to the disease and the proliferation of multidrug-resistant (MDR) strains have created a worldwide interest in expanding current programs in tuberculosis research (*3*). New antimycobacterial agents are needed to treat *Mycobacterium tuberculosis* strains resistant to existing drugs and to shorten the treatment course to improve patient compliance (*4*).

A starting point for this goal has been genomic sequencing. The genome of *M. tuberculosis* is comprised of 4 411 529 base pairs containing 3924 potential open reading frames (*5*). On the basis of sequence homology, biochemical functions have been attributed to ~40% of the predicted proteins, while similarities to other described proteins were found for another 44%, and the remaining 16% bore no resemblance to known proteins and may encode proteins with specific mycobacterial functions (*5*, *6*).

Homologues to enzymes in the purine salvage pathway have been identified in the genome sequence of *M. tuberculosis* (*5*). In the de novo synthesis of purine ribonucleotides, the formation of AMP and GMP from IMP is irreversible, but purine bases, nucleosides, and nucleotides can be interconverted through the activities of purine nucleoside phosphorylase (*deoD*, Rv3307), adenosine deaminase (*add*, Rv3313c), and hypoxanthine−guanine phosphoribosyl transferase (*htp*, Rv3624c). The specific inhibition of *M. tuberculosis* PNP could potentially lead to the accumulation of guanine nucleotides since a putative gua-

† Financial support for this work was provided by the NIH (J.S.B. and V.L.S.), the New Zealand Foundation for Research, Science and Technology (R.H.F. and P.C.T.), and the CNPq and FAPERGS of Brazil (L.A.B. and D.S.S.).

* Corresponding author: phone, (718) 430-3096; fax, (718) 430-8565; e-mail, blanchar@aecom.yu.edu.

‡ Universidade Federal do Rio Grande do Sul.

§ Albert Einstein College of Medicine.

|| Industrial Research, Ltd.

10.1021/bi010584x CCC: $20.00
Published on Web 06/19/2001

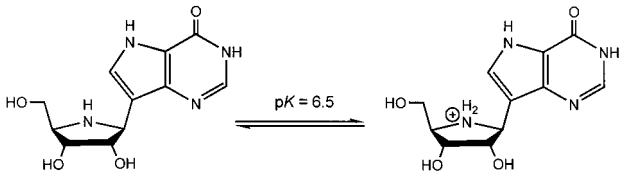

FIGURE 1: Chemical structure of the transition-state analogue ImmH showing protonation of the iminoribitol group. The pK_a for the group is 6.5 (*31*).

nylate kinase (*gmk*, Rv1389) and nucleoside diphosphate kinase (*ndkA*, Rv2445c) are encoded in the genome. The synthesis and degradation of ppGpp, guanosine 3′,5′-bis-(diphosphate), and pppGpp are catalyzed by (p)ppGpp synthase I (*relA*, Rv2583c) using GTP as substrate (*7*). Increased concentration of hyperphosphorylated guanosine moieties is a central feature of a pleiotropic physiological response called the stringent response, through which bacteria enter a latent state in response to nutritional stress (*8*). The accumulation of ppGpp has been implicated in the latency of *M. tuberculosis* (*9*). More recently, it was shown that a *rel*-deficient mutant of *M. tuberculosis* was no longer capable of ppGpp synthesis and that this mutant had impaired long-term survival during in vitro starvation, indicating that ppGpp concentration may control mycobacterial adaptation to growth-limiting conditions, allowing for long-term survival (*10*).

Purine nucleoside phosphorylase (PNP) catalyzes the phosphorolysis of the N-ribosidic bonds of purine nucleosides and deoxynucleosides (*11*). The *M. tuberculosis* PNP shares 34% sequence identity with the human enzyme. Extremely potent transition-state analogues have been developed for mammalian PNP's (*12*) on the basis of the transition-state structure for calf spleen PNP (*13*, *14*). Immucillin-H [ImmH;[1] (1*S*)-1-(9-deazahypoxanthin-9-yl)-1,4-dideoxy-1,4-imino-D-ribitol; Figure 1] possesses features of the transition state that include an elevated pK_a at the N7 position of the 9-deazahypoxanthine (9dHX) ring, a positive charge in the protonated iminoribitol moiety to mimic the ribooxocarbenium ion, and an enzymatically stable carbon−carbon ribosidic bond (*15*). Immucillin-H displays slow-onset inhibition with a 72 pM dissociation constant for human purine nucleoside phosphorylase (*12*). This work identifies ImmH as an even more powerful transition-state analogue for the inhibition of *M. tuberculosis* PNP. Here, we investigate the kinetics of inhibition and the ionic state of ImmH that binds to the enzyme and dissect the binding energetics for the two structural components of the inhibitor, namely, 9dHX and iminoribitol (IR). The three-dimensional structure determination of the *M. tuberculosis* PNP−ImmH complex will guide future efforts to design selective, and potentially more powerful, inhibitors of the mycobacterial enzyme and are reported in the companion paper (*16*).

MATERIALS AND METHODS

Materials. M. tuberculosis H37Rv genomic DNA was a gift from Dr. William R. Jacobs, Jr. (Albert Einstein College of Medicine). Oligonucleotide primers were synthesized by Life Technologies (Gaithersburg, MD). *Nde*I and *Bam*HI restriction enzymes were purchased from New England BioLabs (Beverly, MA), and pET-23a(+) vector DNA and *Escherichia coli* BL21(DE3) cells were from Novagen (Madison, WI). Chromatographic supports were obtained from Pharmacia (Piscataway, NJ). 4×YT medium contained (per liter) 32 g of Bacto tryptone and 20 g of Bacto yeast extract (Difco, Detroit, MI) and 5 g of NaCl, adjusted to either pH 6.0 or pH 7.0 with hydrochloric acid or sodium hydroxide. The substrate 2-amino-6-mercapto-7-methylpurine ribonucleoside (MESG) was the kind gift of Dr. Paul J. Berti (McMaster University, Hamilton, Ontario, Canada).

Cloning and Expression. Two oligonucleotides (5′-CCC-ATATGGCTGACCCGCGCCCCGAT-3′ and 5′-GTGGATC-CTCAGAACCGGGCGATCACGTC-3′) complementary to the amino-terminal coding and carboxy-terminal noncoding strands of the *M. tuberculosis deoD* gene were synthesized to contain *Nde*I and *Bam*HI restriction sites, respectively. The primers were used to PCR amplify the *deoD* gene from *M. tuberculosis* H37Rv genomic DNA using standard PCR conditions (Perkin-Elmer). The PCR product (820 bp) was purified by electrophoresis, digested with *Nde*I and *Bam*HI, and ligated into a pET-23a(+) expression vector which had previously been digested with the same restriction enzymes. The recombinant plasmid was transformed into *E. coli* BL21(DE3) competent cells (Novagen). The DNA sequence of the amplified *M. tuberculosis deoD* was determined to confirm both the identity and integrity of the cloned gene. High-level expression of the *M. tuberculosis* PNP was obtained when the pET-23(+)::*deoD* construct transformed into BL21(DE3) cells was grown at 37 °C in 4×YT medium containing 50 μg/mL carbenicillin at pH 6.0 for 48 h without added IPTG.

Purification of Purine Nucleoside Phosphorylase. Approximately 30 g of cells was collected by centrifugation (6000*g* for 1 h) from 8 L of 4×YT media, pH 6.0, containing 50 μg/mL carbenicillin and stored at −20 °C. All subsequent steps were performed at 4 °C. Frozen cells (30 g) were thawed and suspended in 60 mL of 50 mM tris(hydroxymethyl)aminomethane (Tris), pH 7.6, containing protease inhibitors (Complete protease inhibitor cocktail tablets, Boehringer, Mannheim) and lysozyme (0.2 mg/mL), and the mixture was stirred for 30 min. Cells were disrupted by sonication, and cell debris was removed by centrifugation (40 000*g*, 1 h). Ammonium sulfate was added to a final concentration of 1.0 M and the solution applied to a 2.6 cm × 30 cm phenyl-Sepharose (Pharmacia) column equilibrated in 50 mM Tris (pH 7.6) and 1.0 M $(NH_4)_2SO_4$. The protein was eluted with a 1200 mL linear 1.0 to 0 M $(NH_4)_2SO_4$ gradient. The active fractions were pooled, dialyzed against 50 mM Tris, pH 7.6, for 4 h, and loaded onto a Mono Q HR 16/10 (Pharmacia) anion-exchange column equilibrated with 50 mM Tris, pH 7.6. The protein was eluted with a 200 mL linear 0−0.5 M NaCl gradient, and the active fractions, which exhibited a single band on SDS−PAGE, were pooled. Protein concentrations were estimated by the Bio-Rad protein assay method using bovine serum albumin as the standard.

Molecular Mass Determination. The molecular mass of native *M. tuberculosis* purine nucleoside phosphorylase was estimated by Sephacryl S-200 HR (Pharmacia) gel filtration chromatography and using molecular mass standards (Bio-Rad). The molecular mass standards were detected by

[1] Abbreviations: 9dHX, 9-deazahypoxanthine; ImmH, immucillin-H; IR, iminoribitol; MESG, 2-amino-6-mercapto-7-methylpurine riboside; P_i, inorganic phosphate; PNP, purine nucleoside phosphorylase; RiblP, D-ribose α-1-phosphate.

absorbance at 280 nm, and *M. tuberculosis* PNP was detected by catalytic activity. The subunit molecular mass of the homogeneous enzyme was determined by electrospray ionization mass spectrometry (ESI-MS).

Measurement of Enzyme Activity. Reaction rates were determined by the spectrophotometric method of Webb (*17*), based on the shift in maximum absorbance from 330 nm for MESG to 355 nm for the purine base product. The PNP enzyme activity was followed at 360 nm where, at pH 7.6, the change in extinction coefficient is 11 000 M^{-1} cm^{-1}. Since MESG has a pK_a of 6.5 (*17*), the dependence of the kinetic parameters on pH values ranging from 5.5 to 8.2 was studied utilizing inosine, which has no ionizable groups in this pH range. Absorption spectra of 0.1 mM inosine and hypoxanthine at pH values ranging from 5.2 to 8.8 were obtained in order to determine the pH dependence of the extinction coefficient. The phosphorolysis of inosine to hypoxanthine and ribose was monitored by the change in the UV absorbance at 280 nm using the following molar extinction coefficients: 1020 (pH 5.5), 1000 (pH 6.1, 6.3, 7.0, and 7.5), and 720 (pH 8.2). All enzyme activity measurements were performed at 25 °C using a thermostated Uvikon 9310 spectrophotometer.

Determination of Steady-State Parameters. Steady-state kinetic parameters were determined by varying the concentration of P_i (0.05, 0.1, 0.2, 0.4, 0.8, 1.6, and 2.4 mM) at several fixed concentrations of MESG (10, 20, 30, 50, 100, and 150 μM). Data were plotted in reciprocal form and fitted to the equation for an intersecting initial velocity pattern: $v = k_{cat}AB/(K_{ia}K_b + K_aB + K_bA + AB)$, using the programs of Cleland (*28*), where *A* and *B* are substrate concentrations, K_a and K_b are Michaelis constants for substrates A and B, respectively, and K_{ia} is the dissociation constant for substrate A.

Syntheses of Inhibitors. ImmH, 9dHX, and IR were synthesized by published methods (*29*). The concentrations of ImmH and 9dHX were determined using the published millimolar extinction coefficient of 9.54 at 261 nm at pH 7 for 9-deazainosine (*30*).

Slow-Onset Inhibition. Slow-onset inhibition was measured by the addition of 0.2 nM enzyme to assay mixtures containing near-saturating concentrations of both MESG (500 μM) and P_i (50 mM) in the presence of various ImmH concentrations (2−150 nM). Product formation was followed spectrophotometrically for 3 h. Control experiments contained no inhibitor. Concentrations of the substrates were chosen so that $I_t \gg E_t$ and $I_t \gg K_i^*(1 + A/K_m)$ in order to allow the determination of K_i^* and K_i (*22*). The progress curves were fitted to the integrated equation $P = v_s t + (v_0 - v_S)(1 - e^{-kt})/k$, where v_0, v_S, and k represent respectively the initial velocity, the final steady-state velocity, and the apparent first-order rate constant for the establishment of the equilibrium between EI and EI* complexes (*22*). An estimate of the value for the bimolecular rate constant (k_3) for enzyme−inhibitor association was calculated from the expression $k_3 = k/I$. Values for K_i, which represents the dissociation constant of ImmH from the initially formed E−ImmH complex, and K_i^*, which represents the overall inhibitor dissociation constant for isomerization of the EI complex to EI*, were determined by fitting initial and final steady-state rates, respectively, against inhibitor concentrations to the equations for competitive inhibition as described (*22*). An estimate of K_i was obtained by fitting the variation of initial rate (v_0) with inhibitor concentration (*I*) to the expression $v_0 = (k_{cat}A)/[K_m(1 + I/K_i) + A]$, where *A* denotes the concentration of substrate (MESG), *I* is the concentration of the inhibitory analogue, and K_m is the Michaelis constant for substrate A. K_i^* was determined from fits of the data to $v_S = (k_{cat}A)/[K_m(1 + I/K_i^*) + A]$, where v_S is the final, steady-state, inhibited rate following attainment of equilibrium for the slow-onset step.

Inhibitor Release Studies. M. tuberculosis PNP (60 μM subunits) was preincubated with 60 μM ImmH with and without 50 mM added P_i for 5 h at 25 °C. Control experiments contained no inhibitor. Samples were diluted by factors of 1:250 000 or 1:500 000 into assay mixtures containing 500 μM MESG and 50 mM phosphate buffer, pH 7.6. High substrate concentrations were used to prevent rebinding of ImmH. In these activity regain experiments, the product concentration versus time was fit to the equation $P = v_S t + (v_0 - v_S)(1 - e^{-kt})/k$ (*22*).

Stoichiometry of Inhibition. ImmH (0.5−6 nM) was preincubated with *M. tuberculosis* PNP (6 nM subunits) for 5 h at 25 °C in 56 mM potassium phosphate, pH 7.6. The reactions were initiated by the addition of MESG to a final concentration of 100 μM. Initial rates of product formation were obtained during a linear 2 min reaction time.

Single- and Double-Inhibition Studies. Enzyme activity measurements for the inhibition studies to determine K_i were restricted to the initial rate period for ImmH, 9dHX, and IR. Immucillin-H inhibition was determined at varying concentrations of MESG (10−40 μM) and ImmH (0.4−10 nM) and at a fixed P_i concentration (50 mM). Experimental conditions for the determination of iminoribitol inhibition used varying concentrations of MESG (5−100 μM) and iminoribitol (2−10 μM) at a saturating, fixed P_i concentration of 50 mM. Varying concentrations of MESG (10−60 μM) and 9dHX (0.1−5 μM) at a fixed, saturating P_i concentration of 50 mM were used for 9dHX inhibition studies. The data were fitted to the equation describing competitive inhibition ($v = k_{cat}A/[K_a(1 + I/K_{is}) + A]$) for ImmH and IR and to the noncompetitive inhibition equation ($v = k_{cat}A/[K_a(1 + I/K_{is}) + (1 + I/K_{ii})A]$) for 9dHX using the programs of Cleland (*28*). Double inhibition was performed at varying concentrations of 9dHX (2−20 μM), fixed−varying concentrations of iminoribitol (0−60 mM), and fixed concentrations of MESG (100 μM) and P_i (50 mM). The double-inhibition data were fitted to the following equation for the general case: $1/v = (1/v_0)[1 + I/K_i + J/K_j + IJ/(\beta K_i K_j)]$, where v_0 is the velocity in the absence of inhibitors I and J, K_i and K_j are the apparent dissociation constants, and β is a measure of the degree of interaction of the two inhibitors (*32*).

pH Profiles. The pH dependence of k_{cat} and $k_{cat}/K_{inosine}$ and the competitive inhibition constant for ImmH were determined over the pH range of 5.5−8.2 using variable concentrations of inosine (20−200 μM) and ImmH (0−400 nM), at a fixed, saturating concentration of P_i (50 mM). Reaction mixtures were buffered with 50 mM Tris−phosphate. The pH values were measured in the cuvette after each enzyme reaction using a microelectrode. Reciprocal initial velocities were plotted against reciprocal substrate concentrations at fixed−varying inhibitor concentrations and fitted to the competitive inhibition equation, yielding values for k_{cat}, $k_{cat}/K_{inosine}$, and K_i at different pH values. These parameters were

fitted as a function of pH, using Cleland's program, to the equation describing a decrease in k_{cat}, k_{cat}/K, or inhibition affinities ($1/K_i$) at low pH with a slope of -1 and a plateau at higher pH values: $\log y = \log[c/(1 + H/K_a)]$, where c is the pH-independent plateau value, K_a is the dissociation constant of the group whose ionization decreases the kinetic parameter, and y is either k_{cat}, k_{cat}/K, or $1/K_i$.

RESULTS AND DISCUSSION

Expression, Purification, and Molecular Mass of M. tuberculosis PNP. M. tuberculosis PNP was expressed in *E. coli* after cloning the PCR-amplified *deoD* gene into the pET-23a(+) vector. BL21(DE3) cells transformed with the pET-23a(+)::*deoD* construct overproduced a soluble protein of the expected molecular mass as determined by SDS−PAGE. Following cell lysis, the protein solution containing 1 M $(NH_4)_2SO_4$ was purified by hydrophobic interaction chromatography on phenyl-Sepharose, followed by dialysis and Mono Q anion-exchange chromatography. Approximately 35 mg of homogeneous purine nucleoside phosphorylase was purified 4-fold in 30% overall yield from 30 g of cells. The molecular mass of active *M. tuberculosis* PNP was estimated by gel filtration chromatography to be 80 000 Da. The subunit molecular mass was determined to be 27 437 Da by electrospray ionization−mass spectrometry (ESI-MS), consistent with the posttranslational removal of the N-terminal methionine residue from the full-length gene product (predicted mass: 27 571 Da). The ESI-MS result revealed no peak at the expected mass for *E. coli* PNP (25 950 Da), thus confirming both the identity and the purity of the recombinant protein. The results indicate that *M. tuberculosis* PNP is a trimer in solution, while the oligomeric state of PNP from *E. coli* and *Salmonella typhimurium* is hexameric (*18*).

Catalytic Properties. Initial velocity studies using P_i and MESG as substrates indicated the sequential addition of the two substrates to *M. tuberculosis* PNP. The K_m values for phosphate and MESG were 300 ± 30 and 26 ± 2 μM, respectively. The k_{cat} value of 49 s^{-1} is similar to the turnover number of other trimeric PNP's. *M. tuberculosis* PNP follows Michaelis−Menten kinetics using MESG as substrate, as do other bacterial PNP's (*17*). Cooperative kinetics have been reported with calf spleen (*19*) and human erythrocyte PNP's (*20*, *21*) and have been attributed to nonequivalent active sites (*11*) or a substrate-induced dissociation of the trimer (*19*). The kinetic properties of *M. tuberculosis* PNP allowed ImmH inhibition studies to be performed without complications for both slow-onset inhibition and inhibitor binding stoichiometry studies. In addition, inhibition studies were performed with both 9dHX or IR individually as well as together in double-inhibition studies to probe for synergism in binding.

Slow-Onset Inhibition and Inhibition Constants. Product formation by *M. tuberculosis* PNP in the presence of ImmH exhibits initial rates that decrease as the inhibitor concentration increases, followed by a second, slower rate that is time-dependent (Figure 2). These results are consistent with a two-step mechanism (Scheme 1) in which the inhibitor binds to form a reversible complex, E−P_i−ImmH, that subsequently undergoes a slow isomerization leading to a more tightly bound complex (E*−P_i−ImmH). The progress curves were fitted to the integrated rate equation described in the Materials and Methods section.

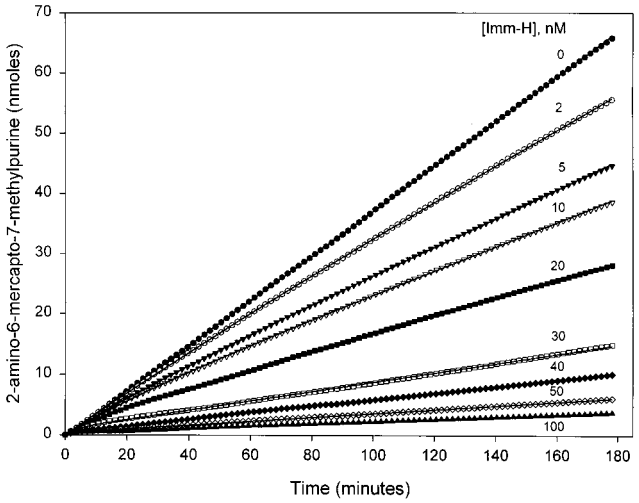

FIGURE 2: Slow-onset binding of ImmH to *M. tuberculosis* PNP. Progress curves were fitted to the equation for slow-onset inhibition as described in Materials and Methods. The lines shown are the fit to the experimental data points.

Scheme 1

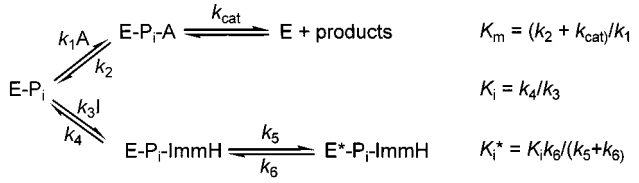

A value of 1.1 ± 0.1 nM for K_i, which represents the rapidly reversible dissociation constant for the PNP−P_i−ImmH ternary complex, was determined from the ImmH effect on the initial rate (v_0) portion of the curve (Figure 3a). This K_i value was confirmed by an independent determination of ImmH inhibition, yielding a value of 2.2 ± 0.3 nM for the linear, competitive inhibition constant (Table 1). A value of 28 (±2) pM for the overall dissociation constant (K_i*) was estimated from the variation of the asymptotic steady-state rate with increasing inhibitor concentration (Figure 3b). The overall dissociation constant (K_i*) is a function of the relative magnitudes of the forward (k_5) and the reverse (k_6) rates for the PNP*−P_i−ImmH isomerization process (Scheme 1). Time-dependent inhibition can only be observed when $K_i^* < K_i$, a condition satisfied only when $k_6 < k_5$ and when k_5 and k_6 are slower than all other steps. Curve fitting the slow-onset data gave values of (0.95 ± 0.23) × 10^{-3} s^{-1} for k_6 and (0.14 ± 0.06) × 10^6 M^{-1} s^{-1} for the bimolecular rate constant (k/I_t) associated with the enzyme and inhibitor interaction. Values $<10^6$ M^{-1} s^{-1} for the bimolecular rate constant indicate a slowly equilibrating enzyme−inhibitor species (*22*).

Inhibitor Release Studies. Strong, noncovalent binding to catalytic sites is a characteristic of transition-state analogue inhibitors. To demonstrate reversible binding, the E*−ImmH and E*−P_i−ImmH complexes were formed by incubation of 60 μM PNP subunits with 60 μM ImmH, in either the absence or presence of 50 mM inorganic phosphate, conditions where most of the inhibitor is bound to the enzyme. Rapid dilution of the E*−ImmH and E*−P_i−ImmH complexes into buffer (1:500) followed by a second dilution into the assay mixture (1:500 or 1:1000) demonstrated the time-dependent, slow release of ImmH in both the presence and

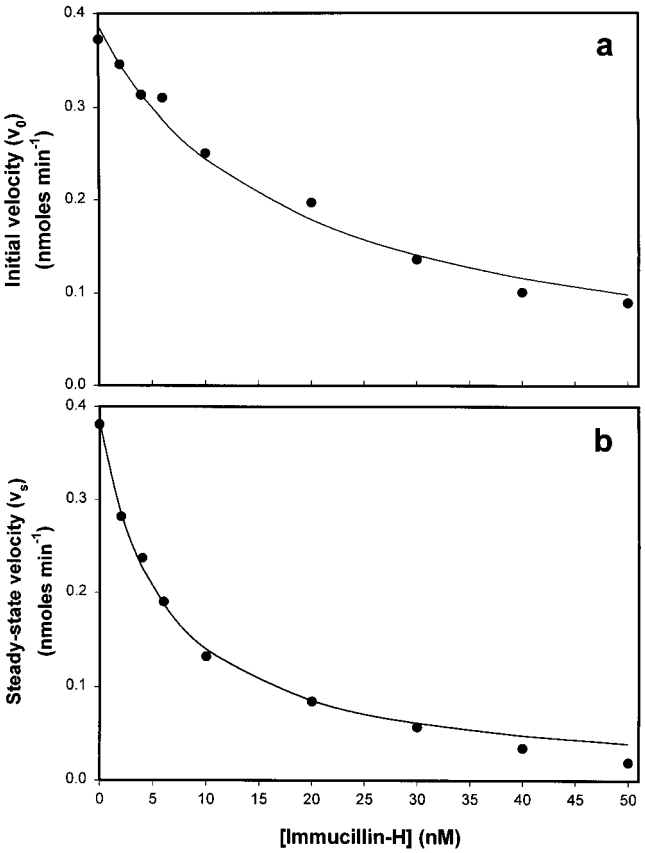

FIGURE 3: Determination of dissociation constants. (a) K_i from a replot of initial rate (v_0) as a function of inhibitor concentration and (b) K_i* from a replot of the final steady-state rate (v_S). The experimental points are values for velocities determined from fits shown in Figure 2. Data analysis as described in Materials and Methods.

Table 1: Kinetic Constants for *M. tuberculosis* PNP

substrate or inhibitor	kinetic constant	value
MESG	K_m	26 ± 2 μM
P_i	K_m	300 ± 30 μM
	k_{cat}	49 ± 2 s^{-1}
ImmH	K_i	2.2 ± 0.3 nM
ImmH	K_i*	28 ± 2 pM
ImmH	$t_{1/2(off)}$	8.4 ± 0.4 min
9dHX	K_{is}	0.39 ± 0.10 μM
9dHX	K_{ii}	0.28 ± 0.03 μM
iminoribitol	K_{is}	2.9 ± 0.3 mM

absence of P_i (Figure 4). The rate of activity regain in the presence of near-saturating concentrations of the substrate, MESG, can be used to estimate the dissociation rate constant k_6 for the complexes (*22*). Values of $(1.37 \pm 0.07) \times 10^{-3}$ s^{-1} and $(1.12 \pm 0.10) \times 10^{-3}$ s^{-1}, in the presence or absence of P_i, respectively, were determined for k_6. As required, the dissociation rate constant, k_6, is independent of enzyme concentration. The value for k_6 in the presence of P_i was independently determined from the progress curves to be $(1.0 \pm 0.2) \times 10^{-3}$ s^{-1}. Inorganic phosphate thus has little effect on the interaction between ImmH and *M. tuberculosis* PNP, consistent with features of the transition state of the mammalian enzyme (*13*). The three-dimensional structure of the calf spleen PNP−7-deazainosine complex confirms that nucleoside binding occurs with this trimeric mammalian PNP in the absence of phosphate (*23*).

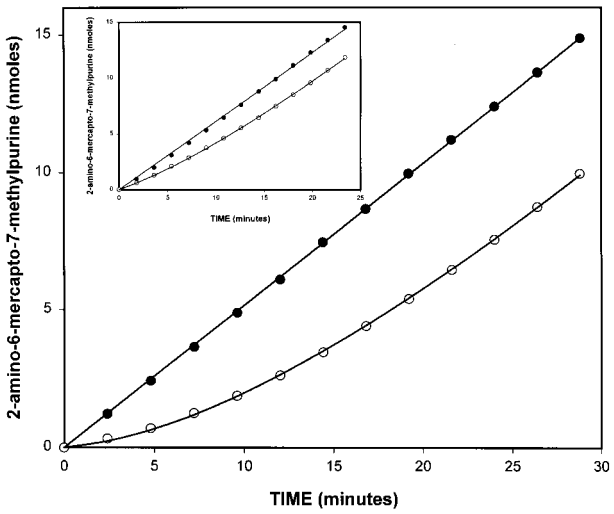

FIGURE 4: Dissociation of ImmH from *M. tuberculosis* PNP. Enzyme (60 μM subunits) and ImmH (60 μM) were incubated for 5 h at 25 °C in either the absence or presence of 50 mM P_i (inset). The control experiment contained no inhibitor. Samples were diluted by factors of 1:250 000 into assay mixtures containing final concentrations of 500 μM MESG and 50 mM phosphate buffer, pH 7.6.

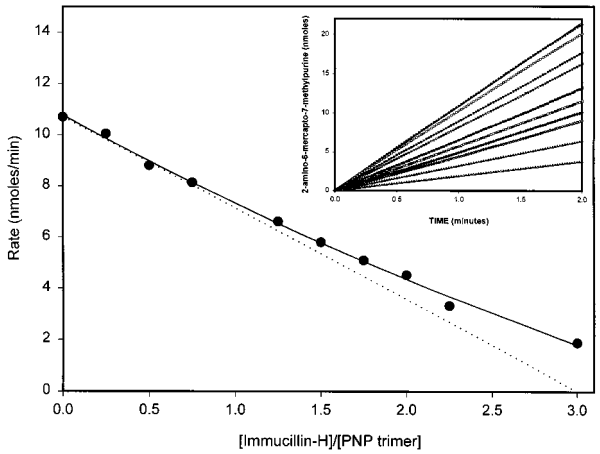

FIGURE 5: ImmH titration of *M. tuberculosis* PNP. Enzyme (6 nM subunits) and inhibitor (0, 0.5, 1, 1.5, 2.5, 3, 3.5, 4, 4.5, and 6 nM) were incubated for 5 h at 25 °C in 56 mM potassium phosphate, pH 7.6. The reactions were initiated by the addition of MESG to a final concentration of 100 μM. Initial rates of product formation were obtained from the 2 min linear progress curves (inset).

The forward rate constant (k_5) was estimated to be 0.11 $\pm$ 0.01 s^{-1} from the relationship $k_5 = k_6(K_i/K_i^* - 1.0)$ (*22*). The equilibrium constant for the E−P_i−ImmH to E*−P_i−ImmH isomerization, k_5/k_6, is 80.3. The E*−P_i−ImmH complex is thus −2.6 kcal/mol more stable than the initially formed E−P_i−ImmH complex. The half-time for inhibitor dissociation from the E*−P_i−ImmH ternary complex ($t_{1/2}$ = 8.4 min) and the isomerization equilibrium constant will determine the in vivo effectiveness of the inhibitor. The slow release of bound inhibitor from the E*−P_i−ImmH complex allows the stoichiometry of inhibitor binding to be determined. After a 5 h preincubation at various [ImmH]/$[PNP]_{trimer}$ ratios, the initial rates of product formation were determined (Figure 5). The results establish that the trimeric *M. tuberculosis* PNP binds three molecules of ImmH, with equal affinity, in contrast to one-third-of-the-sites binding

and inhibition observed for both calf spleen and human PNP's (*11*).

ImmH was designed from the experimentally determined transition-state structure for bovine PNP's (*13*, *14*). The similarities between the inhibition constants for ImmH with the *M. tuberculosis* and bovine PNP's (28 and 23 pM, respectively) suggest similar dissociative transition states for both enzymes. Alignment of amino acid sequences of mammalian and *M. tuberculosis* PNP's reveals the strong conservation of amino acid residues involved in binding and catalysis (*16*). The three-dimensional structures of bovine spleen PNP (*23*−*25*), human erythrocyte PNP (*26*, *27*), and the *M. tuberculosis* PNP reveal almost identical amino acid contacts in the catalytic sites of all three enzymes.

Given these sequence similarities, it is interesting to compare the ImmH inhibition of *M. tuberculosis* PNP to that previously reported for bovine and human PNP (*12*). The K_i value for ImmH observed for the *M. tuberculosis* enzyme (1−2 nM) is almost 20−40 times lower than that observed for bovine PNP (41 nM), indicating stronger ground-state interactions with the *M. tuberculosis* enzyme. In contrast, the forward and reverse rates of E−P_i−ImmH to E*−P_i−ImmH isomerization are much faster for the *M. tuberculosis* enzyme (0.1 s^{-1} and 1.4 × 10^{-3} s^{-1}, respectively) than the bovine PNP (6.4 × 10^{-2} s^{-1} and 4 × 10^{-5} s^{-1}, respectively) (Table 1). The slow isomerization of bovine PNP has been ascribed to structural rearrangements of residues, including surface loops that are mobile in the unliganded enzyme but immobile in the structurally characterized bovine PNP−ImmH complex. Fortuitously, the K_i* values for ImmH are nearly equivalent at 23 and 28 pM for bovine and *M. tuberculosis* PNP's while the interaction with human PNP is slightly weaker at 72 pM (*12*). In the accompanying paper, the PNP−ImmH structure is shown to differ considerably from mammalian PNP's in subunit interface contacts, a possible explanation for these results. Despite these differences, the similar K_i* and k_{cat} values for mammalian and *M. tuberculosis* enzymes suggest similar transition-state interactions.

Initial Velocity Inhibition Studies. Iminoribitol displayed a slope-linear, competitive pattern with an estimated K_{is} value of 2.9 (±0.3) mM versus MESG at a saturating concentration of P_i (Table 1). 9-Deazahypoxanthine exhibited linear, noncompetitive inhibition versus MESG with values of 0.39 (±0.10) μM for K_{is} and 0.28 (±0.03) μM for K_{ii} (Table 1). The noncompetitive inhibition displayed by 9dHX suggests that binding occurs to both the free enzyme and the PNP−Rib1P complex after release of the 2-amino-6-mercapto-7-methylpurine base. Double inhibition is a method of detecting synergism in the binding of two inhibitors (*32*). The double-inhibition measurements displayed a crossover point below the horizontal axis (Figure 6a), indicating that the inhibitors can bind to the same form of the enzyme. Analysis of these results yielded a β value of 13 (±1). Since β is a measure of the degree of interaction of the two inhibitors and values of $\beta > 1$ indicate antagonistic binding, the double-inhibition results demonstrate that formation of the PNP−P_i−9dHX−IR dead-end ternary complex occurs and that their binding is neither exclusive nor synergistic. Experimental determination of these three parameters provides a calculated value of 5.1 μM for the dissociation constant of 9dHX from the PNP−P_i−9dHX−IR complex. Since these are three of the four coupled dissociation constants of a thermodynamic box, a value of 38 mM was estimated for the dissociation constant of iminoribitol from the PNP−P_i−9dHX−IR complex (Figure 6b). The structural comparison between *M. tuberculosis* complexes of PNP−ImmH−P_i and PNP−9dHX−IR−P_i reveals that binding of the components of ImmH causes a disruption of the hydrogen bond network. The van der Waals contact between C9 of 9dHX and Cl′ of iminoribitol in the quaternary complex forces a separation of iminoribitol and phosphate in the active site (*16*). As a consequence, several of the favorable hydrogen bonds found in the complex of PNP−ImmH−P_i are weakened. These changes account for the antagonistic binding observed in double-inhibition experiments.

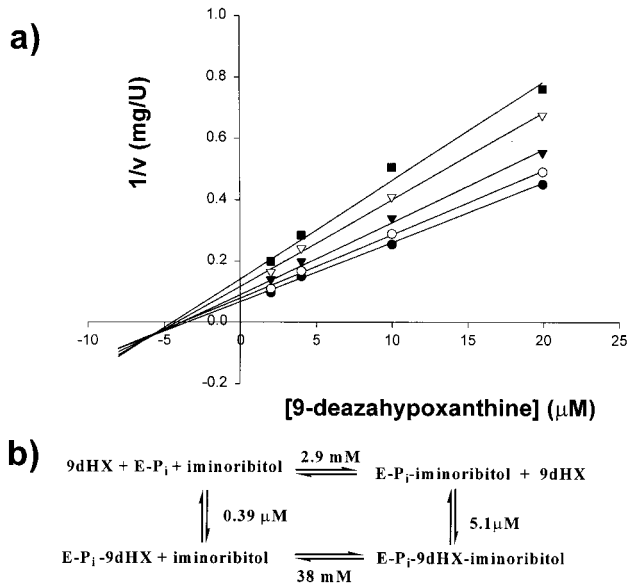

FIGURE 6: (a) Double inhibition by 9dHX and iminoribitol. The inhibition pattern as a function of varied 9dHX concentration, at fixed concentrations of MESG (100 μM) and P_i (50 mM), was obtained at fixed−varying concentrations of iminoribitol (● = 0 mM, ○ = 10 mM, ▼ = 20 mM, ▽ = 40 mM, ■ = 60 mM). The lines through the data represent the best fit to the equation $1/v = (1/v_0)[1 + I/K_i + J/K_j + IJ/(\beta K_i K_j)]$, yielding a value of $\beta = 13 \pm 1$. (b) Coupled dissociation constants for inhibitor binding to *M. tuberculosis* PNP. A value of 38 mM was calculated for the dissociation constant of iminoribitol from the PNP−P_i−9dHX−IR complex.

pH Profiles. As pH decreases, k_{cat}, k_{cat}/K_m, and the affinity for ImmH ($1/K_i$) all decrease as the consequence of the protonation of an ionizable group. The log of k_{cat} decreases at low pH as a single group with a pK_a value of 6.05 ± 0.11 is protonated (Figure 7). Analysis of log k_{cat}/K_m versus pH yielded a pK_a value of 6.29 ± 0.02 (Figure 7). Since inosine contains no ionizable functions over the pH range studied, the pK_a values of 6.29 and 6.05 can be assigned to an ionizable group in the enzyme−P_i complex and to a group in the enzyme−inosine−P_i complex which is required to be unprotonated for catalysis. The crystal structure of *M. tuberculosis* PNP in complex with ImmH and P_i shows that the oxocarbenium transition state for phosphorolysis is stabilized by an interaction with the 5′-OH group, and this group interacts with His243 through a 2.5 Å hydrogen bond (Figure 7 in ref *16*). His243 is conserved in mammalian PNP's. However, conversion of this group to an Ala in human PNP decreases k_{cat} only by a factor of 4 and k_{cat}/K_m by a factor of 20 (*27*). Therefore, His243 may not be the

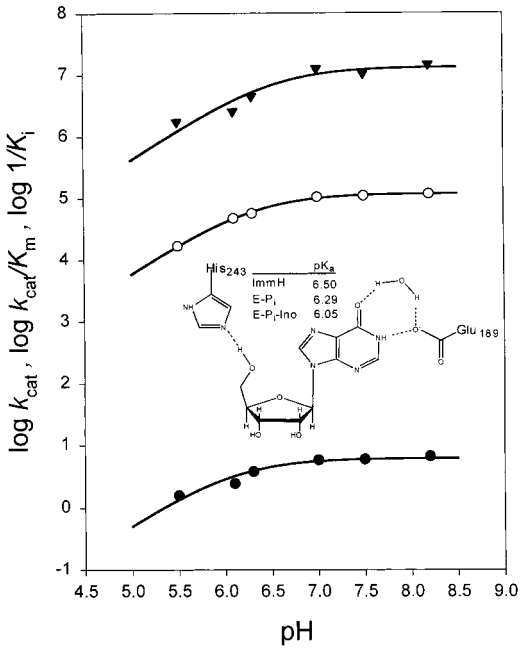

FIGURE 7: pH dependence of kinetic parameters for inosine phosphorolysis and the ImmH inhibition constant. The lines through the data represent the best fit to the equation describing a decrease in the value of the kinetic constant at low pH with a slope of −1 and a plateau at higher pH values: $\log y = \log[c/(1 + H/K_a)]$, where y represents either k_{cat}, k_{cat}/K, or $1/K_i$. Plots: (●) log k_{cat}, (○) log $k_{cat}/K_{inosine}$, and (▼) log $1/K_i$. (Inset) $k_{cat}/K_{inosine}$ and k_{cat} versus pH analysis yielded pK_a values of 6.29 and 6.05 assigned respectively to the unprotonated form of the imidazole ring of His243 or Glu189 in the free enzyme and the enzyme−substrate complex.

group observed in the pK_a profiles. A second ionizable group in the active site is Glu189 that contacts N1 and a water proposed to protonate O6 (Figure 7). Glu189 is also conserved in mammalian PNP's and mutation of this residue to Ala in human PNP decreases k_{cat} by a factor of 14 and k_{cat}/K_m by a factor of 3000 (*27*). Protonation of this group prevents the substrate binding interaction at N1 and the proton-transfer bridge responsible for O6 protonation at the transition state (*33*). Glu189 is a likely candidate for the group whose ionization is observed in the pK_a profiles of k_{cat} and k_{cat}/K_m. Inosine is a neutral molecule, while the transition state for PNP carries a net positive charge, which is delocalized through the ribosyl and purine rings (*15*). The $1/K_i$ for ImmH decreased at low pH as a result of the protonation of a single ionizable group with a pK_a value of 6.5 ± 0.1 (Figure 7). Titrations of ImmH with acid/base cycles and proton NMR analyses have established a pK_a value of 6.5 for formation of the N4′ iminoribitol monocation (Figure 1, *33*). The pK_i profile suggests[2] that ImmH binds to the enzyme as the neutral species, mimicking the substrate. Subsequent inhibitor distortion results in the formation of the C5′−OH−N4′ interaction, followed by the protonation of the N4′ nitrogen to generate the tight-binding form of the inhibitor, which is −2.6 kcal/mol more stable than the rapidly formed initial inhibitor complex (K_i^* = 28 pM and K_i = 2.2 nM). A proton relay pathway from solvent to this His243 may be involved in this process, as described in the X-ray crystal structure of these complexes (*16*.

Summary and Conclusions. M. tuberculosis expresses a trimeric PNP that is susceptible to inhibition by ImmH, a slow-onset tight-binding transition-state analogue. The pH dependence of inhibition indicates that ImmH binds to the enzyme as the neutral form followed by a slow conformational change, presumed to be protonation to form an oxocarbenium ion analogue of the transition state. Glu189 is a candidate residue whose protonation affects the pH dependence of catalysis and is involved in both substrate binding and proton transfer to form the transition state. Division of ImmH into its component pieces reveals that the 9-deazahypoxanthine moiety binds 7000 times more tightly than iminoribitol, and ImmH binds 14 000 times tighter than 9-deazahypoxanthine. Forcing the separate components of ImmH into the catalytic site antagonizes tight binding. Thus, leaving group interactions dominate transition-state analogue binding, and the integrity of the transition-state inhibitor molecule is required for full binding interactions.

[2] Although we favor this interpretation, these data alone cannot distinguish between the unprotonated inhibitor binding to protonated enzyme and protonated inhibitor binding to unprotonated enzyme.

REFERENCES

1. Raviglione, M. C., Snider, D. E., Jr., and Kochi, A. (1995) *JAMA, J. Am. Med. Assoc. 273*, 220−226.
2. Stokstad, E. (2000) *Science 287*, 2391.
3. Barkley, W. E., and Kubica, G. P. (1994) in *Tuberculosis: Pathogenesis, Protection, and Control* (Bloom, B. R., Ed.) pp 61−71, American Society for Microbiology, Washington, DC.
4. Parrish, N. M., Dick, J. D., and Bishai, W. R. (1998) *Trends Microbiol. 6*, 107−112.
5. Cole, S. T., Brosch, R., Parkhill, J., Garnier, T., Churcher, C., Harris, D., Gordon, S. V., Eiglmeier, K., Gas, S., Barry, C. E., Tekaia, F., Badcock, K., Basham, D., Brown, D., Chillingworth, T., Connor, R., Davies, R., Devlin, K., Feltwell, T., Gentles, S., Hamlin, N., Holroyd, S., Hornsby, T., Jagels, K., Krogh, A., McLean, J., Moule, S., Murphy, L., Oliver, K., Osborne, J., Quail, M. A., Rajandream, M.-A., Rogers, J., Rutter, S., Seeger, K., Skelton, J., Squares, R., Squares, S., Sulston, J. E., Taylor, K., Whitehead, S., and Barrell, B. G. (1998) *Nature 393*, 537−544.
6. Editorial (2000) *Nat. Struct. Biol. 7*, 87−88.
7. Avarbock, D., Salem, J., Li, L., Wang, Z., and Rubin, H. (1999) *Gene 233*, 261−269.
8. Cashel, M., Gentry, D. R., Hernandez, V. J., and Vinella, D. (1996) in *Escherichia coli* and *Salmonella* cellular and molecular biology (Neidhardt, F. C., Ed.) pp 1458−1496, American Society for Microbiology, Washington, DC.
9. Ojha, A. K., Muckherjee, T. K., and Chatterji, D. (2000) *Infect. Immun. 68*, 4084−4091.
10. Primm, T. P., Andersen, S. J., Mizrahi, V., Avarbock, D., Rubin, H., and Barry, C. E., III (2000) *J. Bacteriol. 182*, 4889−4898.
11. Parks, R. E., Jr., and Agarwal, R. P. (1972) *Enzymes 7*, 483−514.
12. Miles, R. W., Tyler, P. C., Furneaux, R. H., Bagdassarian, C. K., and Schramm, V. L. (1998) *Biochemistry 37*, 8615−8621.
13. Kline, P. C., and Schramm, V. L. (1993) *Biochemistry 32*, 13212−13219.
14. Kline, P. C., and Schramm, V. L. (1995) *Biochemistry 34*, 1153−1162.
15. Schramm, V. L. (1998) *Annu. Rev. Biochem. 67*, 693−720.
16. Shi, W., Basso, L. A., Santos, D. S., Tyler, P. C., Furneaux, R. H., Blanchard, J. S., Almo, S. C., and Schramm, V. L. (2001) *Biochemistry 40*, 8204−8215.
17. Webb, M. R. (1992) *Proc. Natl. Acad. Sci. U.S.A. 89*, 4884−4887.
18. Jensen, K. F., and Nygaard, P. (1975) *Eur. J. Biochem. 51*, 253−265.

19. Ropp, P. A., and Traut, T. W. (1991) *J. Biol. Chem. 266*, 7682−7687.
20. Kim, B. K., Cha, S., and Parks, R. E., Jr. (1968) *J. Biol. Chem. 243*, 1771−1776.
21. Agarwal, K. C., Agarwal, R. P., Stoeckler, J. C., and Parks, R. E., Jr. (1975) *Biochemistry 14*, 79−84.
22. Morrison, J. F., and Walsh, C. T. (1988) *Adv. Enzymol. Relat. Areas Mol. Biol. 61*, 201−301.
23. Mao, C., Cook, W. J., Zhou, M., Federov, A. A., Almo, S. C., and Ealick, S. E. (1998) *Biochemistry 37*, 7135−7146.
24. Bzowska, A., Luic, M., Schroder, W., Shugar, D., Saenger, W., and Koellner, G. (1995) *FEBS Lett. 367*, 214−218.
25. Koellner, G., Luic, M., Shugar, D., Saenger, W., and Bzowska, A. (1997) *J. Mol. Biol. 265*, 202−216.
26. Ealick, S. E., Rule, S. A., Carter, D. C., Greenhough, T. J., Babu, Y. S., Cook, et al. (1990) *J. Biol. Chem. 265*, 1812−1820.
27. Erion, M. D., Takabayashi, K., Smith, H. B., Kessi, J., Wagner, S., Honger, S., Shames, S. L., and Ealick, S. E. (1997) *Biochemistry 36*, 11725−11734.
28. Cleland, W. W. (1979) *Methods Enzymol. 63*, 103−138.
29. Evans, G. B., Furneaux, R. H., Gainsford, G. J., Schramm, V. L., and Tyler, P. C. (2000) *Tetrahedron 56*, 3053−3062.
30. Lim, M.-I., Ren, W.-Y., Otter, B. A., and Klein, R. S. (1983) *J. Org. Chem. 48*, 780−788.
31. Horenstein, B. A., and Schramm, V. L. (1993) *Biochemistry 32*, 9917−9923.
32. Cleland, W. W. (1990) *Enzymes 19*, 99−158.
33. Fedorov, A., Shi, W., Kicska, G., Fedorov, E., Tyler, P. C., Furneaux, R. H., Hanson, J. C., Gainsford, G. J., Larese, J. Z., Schramm, V. L., and Almo, S. C. (2001) *Biochemistry 40*, 853−860.

BI010584X